CHEMICAL ENGINEERING TRANSACTIONS

VOL. 76, 2019

A publication of AIDIC

The Italian Association of Chemical Engineering
Online at www.aidic.it/cet

Guest Editors: Petar S. Varbanov, Timothy G. Walmsley, Jiří J. Klemeš, Panos Seferlis

ISBN 978-88-95608-73-0; **ISSN** 2283-9216

DOI: 10.3303/CET1976040

Numerical Study of Flow and Heat Transfer in Gravity-Driven Particle Flow Around a Circular or Elliptical Tube

Xing Tian[a], Jian Yang[a,b,*], Zhigang Guo[a], Qiuwang Wang[a], Bengt Sunden[b]

[a]Key Laboratory of Thermo-Fluid Science and Engineering, MOE, School of Energy and Power Engineering, Xi'an Jiaotong University, Xi'an, Shaanxi, 710049, P.R. China
[b]Department of Energy Sciences, Lund University, Lund 22100, Sweden
yangjian81@mail.xjtu.edu.cn

Gravity flowing beds of particles are widely found in chemical engineering industries, where the particle flow and heat transfer inside are very important for high efficiency and safe operations in the relevant facilities. In the present study, the particle flow around a circular or elliptical tube is numerically investigated with the discrete element method (DEM), where the particle flow and heat transfer in different zones around the tube are carefully analyzed. According to the particle flow and geometric characteristics of the tube, eight particle flow zones are established around the tube. It is found that the pore structure, contact number and velocity of particles in different particle flow zones are different due to the size of the stagnation zone and cavitation zone at the top and bottom of the tube. Compared with the circular tube, the porosity in the region of $R < 2\ d_p$ outside the elliptical tube is smaller in zone 1, 3 and 4. The contact number in zones 3 and 4 are almost 1.3 and 1.5 times of that of the circular tube respectively, and the particle velocity in the stagnation zone is larger. Finally, based on the flow characteristics of particles around the two kinds of tubes, the heat transfer performance of the two kinds of tubes in different zones is analyzed. Due to the improvement of flow performance around the elliptical tube, the heat transfer performance of the elliptical tube is better than that of the circular tube.

1. Introduction

In the past 30 years, China's energy and environmental problems have become increasingly prominent (Gen et al., 2018), which makes improving the energy efficiency and sustainable energy development very important (Subash et al., 2018). Nowadays, the waste heat of high temperature solid bulk annually produced by industry is quite huge (Zhao et al., 2016). In order to improve energy efficiency, a variety of physical and chemical methods have been developed to recover waste heat from bulk materials (Zhang et al., 2013). Moving Bed Heat Exchanger (MBHE) is being implemented gradually due to its low cost and clean energy. How to obtain heat from particles efficiently and control the flow pattern of particles is a key problem in MBHE.
For gravity-driven particle flow and heat transfer, many researchers have carried out experimental and simulation studies. Duan et al. (2018) proposed a multi-stage slag waste heat recovery system to increase the utilization rate of blast furnace slag waste heat. The results showed that, the multi-stage slag waste heat recovery system has excellent application potential in energy saving. Zheng et al. (2018) studied the heat transfer of calcined petroleum coke and a heat exchanger tube by numerical simulation. It was found that the contact conduction between particles was dominant and the contribution of gas heat transfer was small. Liu et al. (2015) studied the heat transfer characteristics of the gravity bed waste heat boilers by experiments, and discussed the effects of particle diameter and particle velocity on the heat transfer coefficient and recovery rate. Baumann et al. (2015) studied the influence of different tube bundle arrangement on the heat transfer performance of MBHE by experiments.
Most of the studies mentioned above focus on the macroscopic heat transfer characteristics of the MBHE. In order to explain the particle flow around the tube and heat transfer in detail, the relationship between particle flow and heat transfer in the MBHE can be anticipated by means of numerical simulation. The purpose of this study is to compare the flow and heat transfer characteristics of gravity-driven particle flow around a single circular tube and an elliptical tube. The discrete element method (DEM) with the heat transfer model is used in

Paper Received: 12/03/2019; Revised: 24/04/2019; Accepted: 25/04/2019
Please cite this article as: Tian X., Yang J., Guo Z., Wang Q., Sunden B., 2019, Numerical Study of Flow and Heat Transfer in Gravity-Driven Particle Flow Around a Circular or Elliptical Tube, Chemical Engineering Transactions, 76, 235-240 DOI:10.3303/CET1976040

the numerical simulation. The flow and heat transfer performances of particles around the tube in different flow zones are analyzed. In addition, the relationship between the particle flow characteristics and heat transfer is discussed. This work is helpful to understand the characteristic of particle flow and heat transfer around different tubes, which also help the design and optimization of the MBHE in the future.

2. Method and simulation

2.1 Method

Gravity-driven particle flow is a two-phase flow, and particles in MBHE accumulate tightly and flow slowly. The internal gas flow is mainly driven by particles. Comparing with the drag force between particles and gas, the stress between particles dominates. Srivastava et al. (2003) pointed out that the influence of gas flow on particle flow is very small, and the gas convection in heat transfer can be neglected (Hou et al., 2016). Therefore, in the present research, the flow and heat transfer in the solid phase is mainly concerned, and the flow of gas is neglected. The present simulation is carried out by EDEM2.6 and the heat transfer model described below is added to EDEM to obtain the heat transfer characteristics of particles.

In the present research, the heat conduction between particles and walls is mainly considered. The thermal resistance model adopted in this paper is based on the following assumptions: 1) the particle flow is composed of spherical particles with the same diameter; 2) the heat capacity of gas between particles is negligible, and the temperature of an individual particle is uniform; 3) the particles are surrounded by a gas film, and the film thickness is 0.1 d_p; 4) the heat transfer path between particles is along the radial direction of the particle; 5) the physical properties are kept constant; 6) thermal radiation and convection heat transfer are not considered. In the present study, the main thermal resistances are internal thermal resistance, contact thermal resistance and gas film thermal resistance between particles (Guo et al., 2018).

2.2 Simulation

The physical model is shown in Figure 1. The wall effect has been taken into account, and the geometric sizes are selected according to the study of Zhang et al. (2017), where the particle diameter (d_p) is 3 mm. The major axis of the elliptical tube is equal to the diameter of the circular tube, and the minor axis of the elliptical tube is half of the circular tube diameter. Typical geometric and physical parameters are given in Table 1, where the physical properties are the same as those of Liu et al. (2015). During the simulations, the tube wall temperature is constant and the other walls in the channel are adiabatic. The velocity of particles in the channel is controlled at the outlet, as described by Baumann et al. (2015) and kept constant in the vertical direction.

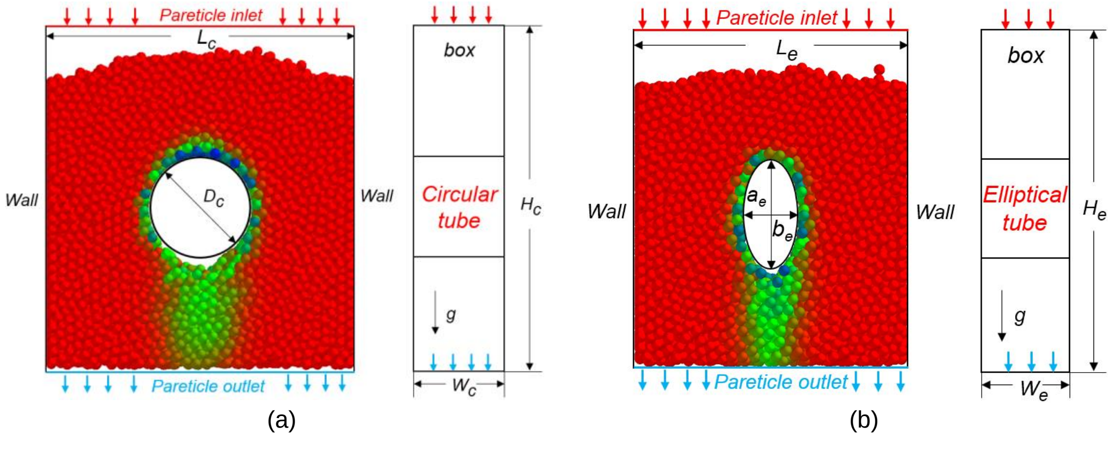

Figure 1: Geometry model of particle flow around (a) Circular tube and (b) Elliptical tube

During the simulation process, the random packing and high temperature particles are generated in the channel at initial. Particles begin to flow with control in outlet and are cooled by the tube wall. The heat transfer to different tube zones is counted over time during simulation. Particles leaving the channel from the outlet enter the channel from the inlet with updated temperature, which makes the number of particles in the channel constant. The overall simulation lasts 60 s and the heat Q in finally 30 s is analyzed, when Q have almost changed linearly. The formula of the heat transfer coefficient is shown by Eq, (1), where Q is the total heat amount transferred between particles and tube wall. The heat transfer coefficients obtained from the simulation are compared with the experimental data (Liu et al. 2015) to validate the heat transfer model, as shown in Figure 2(a). The simulation results are in good agreement with the experimental data. The maximum and the average deviations of the heat transfer coefficient are 10.5 % and 6.03 %, respectively, which shows that the heat transfer model used in DEM is reasonable.

$$h = \frac{Q}{A_{\text{tube}}\left(T_{\text{in}} - T_{\text{tube}}\right)\Delta t} \tag{1}$$

Table 1: Main parameters in simulation

name	parameter	value	name	parameter	value
	L_c/ L_e (m)	0.09/0.074		ρ/(kg/m^3)	2848
	W_c/W_e (m)	0.03/0.03		C_p/(J·kg^{-1}·K^{-1})	1210
geometry	H_c/H_c (m)	0.09/0.078	particle	k_p/(W·m^{-1}·K^{-1})	0.55
	D_c/a_e/b_e(m)	0.03/0.03/0.015		E/(Pa)	2.2*10^8
	T_{tube}/(K)	300		T_{in}/(K)	700
gas	k_f /(W·m^{-1}·K^{-1})	0.0257	time step	Δt/(s)	2.6*10^{-6}

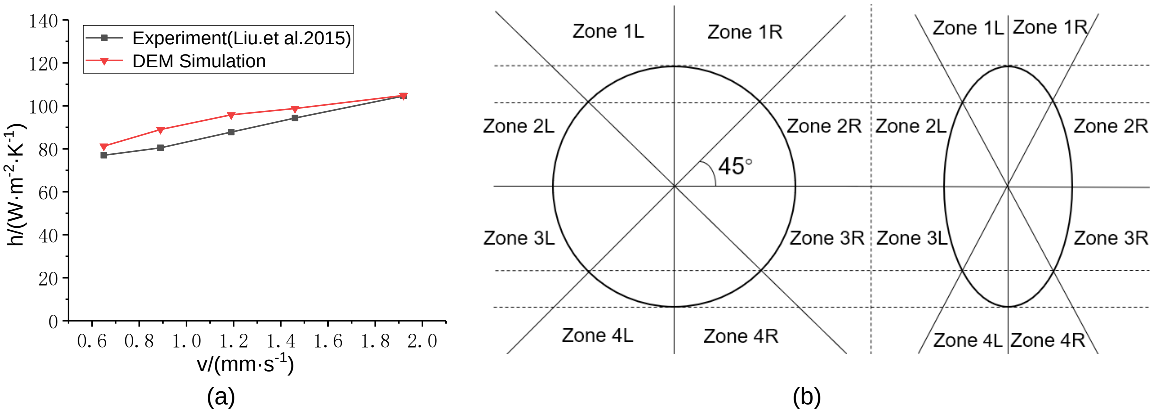

Figure 2: Model validation (a) and Zone division outside the tube (b)

3. Results and discussion

In order to clearly demonstrate the variation of the particle flow and heat transfer near the tube wall, the region outside the circular tube is divided into eight zones each with an angle of 45°. The height of the dividing point of different zones for the elliptical tube is kept the same as that of the circular tube, as shown in Figure 2(b). The particle outlet velocities for different simulation cases are shown in Table 2.

Table 2: Outlet particle velocities for different simulation cases

Case	1	2	3	4	5	6	7	8
Velocity (mm/s)	0.5	1	2	4	8	12	16	20

3.1 Time-averaged porosity characteristics

The variation of the time-averaged porosity in different zones perpendicular to the wall direction outside the circular and elliptical tubes is shown in Figure 3 for the simulated case 1. R is the radial distance from a point outside the tube to the tube wall, and r is the distance from a point outside the tube to the tube center. Due to the symmetrical structure of the tube, the flow characteristics on both sides of the tube are identical. Therefore, only the porosity distribution on the left side of the tube is given. When particles flow around a circular tube, the porosity gradient distribution is obvious in the region of R < 2 d_p, and the porosity decreases gradually along the flow direction as shown in Figure 3(a). In the region of R > 2 d_p, the porosity of different zones fluctuates in a small range. Zone 1 has the smallest porosity near the tube wall because of the stagnation zone formed by the obstruction of the tube and the gravity action of the particles. At zone 4, the particles contact intermittently with part of the tube wall, which has the largest porosity near the wall. The cavitation zone is formed here. When particles flow around an elliptical tube, the porosity of zones 1, 2 and 3 are close to each other in the region of

R < 2 d_p, and the porosity gradient is not obvious as shown in Figure 3(b). In the region of R > 2 d_p outside the elliptical tube, the porosity tends to the same fixed value, which is the same as that of the circular tube. For two kinds of tubes, the pore structure of the particle flow near the wall of zones 1, 2 and 3 (R < 2 d_p) is affected by the wall effect, and the porosity curve fluctuates regularly near the wall. Because of the influence of the cavitation zone, the porosity curve of zone 4 varies almost linearly in the region of R < 1.5 d_p.

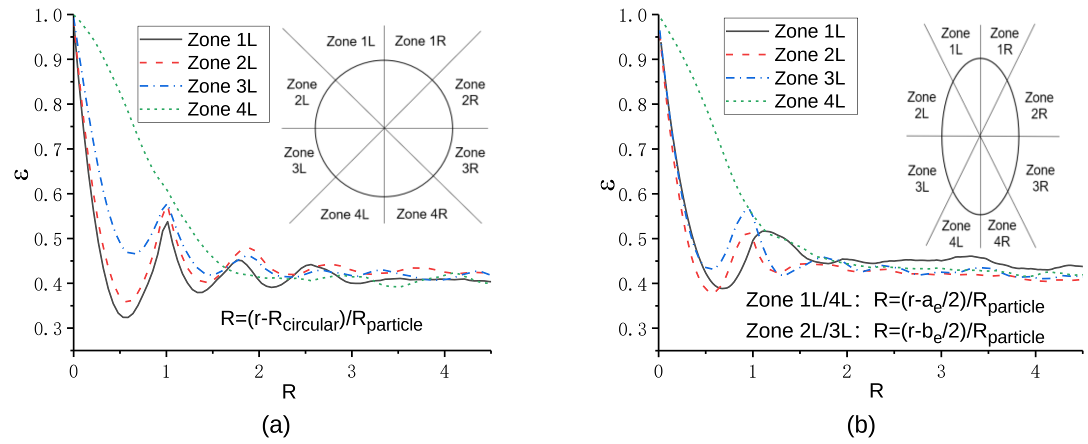

Figure 3: Time-averaged porosity curve of particle flow outside Circular tube (a) and Elliptical tube (b)

3.2 Contact characteristics and average velocity variations

The contact number is the amount of particles in contact with the tube wall per unit area. Figure 4 shows the contact number results at different cases in different zones. For the circular tube, the contact numbers in zone 1 and zone 2 are similar. In zone 3, because of the sparse rheology of particles, the contact number is smaller than that in zones 1 and 2. Zone 4 has the lowest contact number due to the influence of the cavitation zone, and the contact number is about 12 % of that of zone 1. For the elliptical tube, the contact number of particles in zone 1, zone 2 and zone 3 are similar. The contact numbers in zones 3 and 4 are 130 % and 150 % larger than that of the circular tube. Compared with the circular tube, the contact between particles and the elliptical tube wall is better and the elliptical tube cavitation zone is smaller.

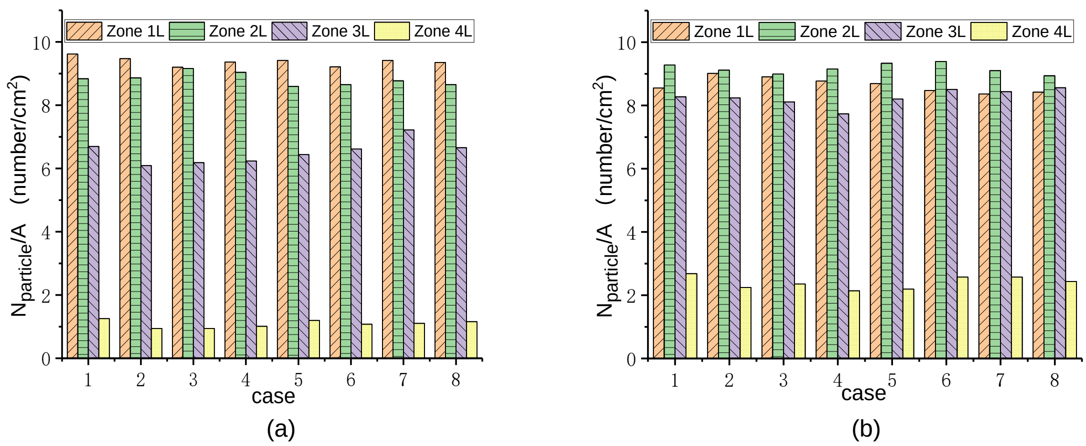

Figure 4: Contact Number of Circular tube (a) and Elliptical tube (b)

The percentage of the average velocity of particles in contact with the tube wall in different zones with different cases is shown in Figure 5. As seen from the Figure 5, the average velocity between different zones has a significant gradient. The particle velocity is much less than the outlet velocity in zone 1, and the stagnation zone is formed here. The average velocity of the circular tube and the elliptical tube in zone 1 is 9% and 25% of the particle outlet velocity respectively ,which means that the particle renewal in the elliptical tube stagnation zone is faster than that of the circular tube. Besides, the particle velocity in zone 2 is almost equivalent to the particle outlet velocity. As for zone 3, the average velocity is affected by the cavitation zone and the gravity action of particles. The average velocity in this zone is much faster than the outlet velocity. The particle velocity of the circular tube and the elliptical tube in zone 3 is 185% and 152% of the particle outlet velocity respectively. The velocity distribution around the elliptical tube is more uniform.

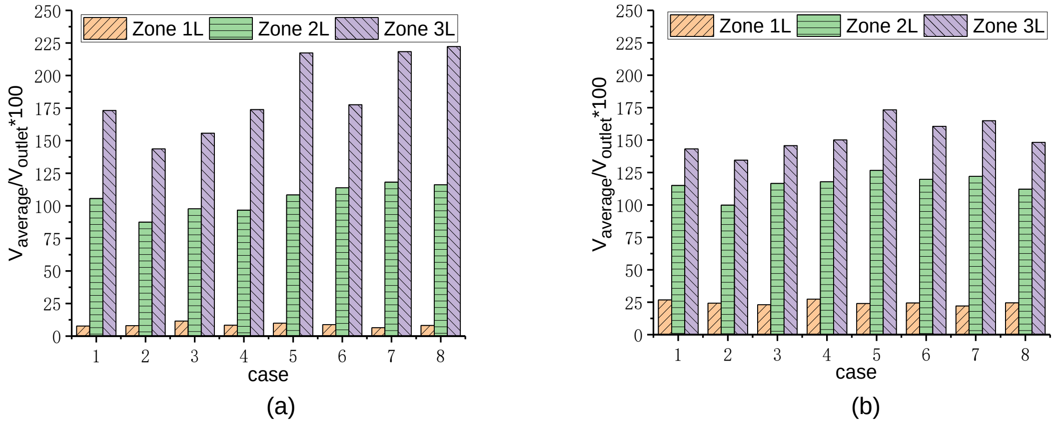

Figure 5: Average particle flow velocity of Circular tube (a) and Elliptical tube (b)

3.3 Heat transfer characteristics

The heat transfer coefficients in different zones with different cases are shown in Figure 6. Zone 4 has the lowest heat transfer coefficients because of the cavitation zone. Compared with zones 1 and 2, zone 3 has a larger porosity and a lower contact number. Therefore, the heat transfer coefficient is lower.

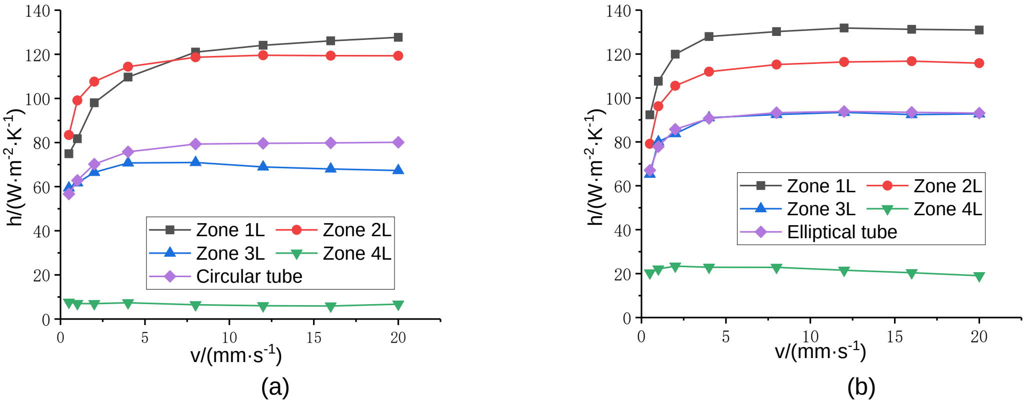

Figure 6: Heat transfer coefficients in different zones of Circular tube (a) and Elliptical tube (b)

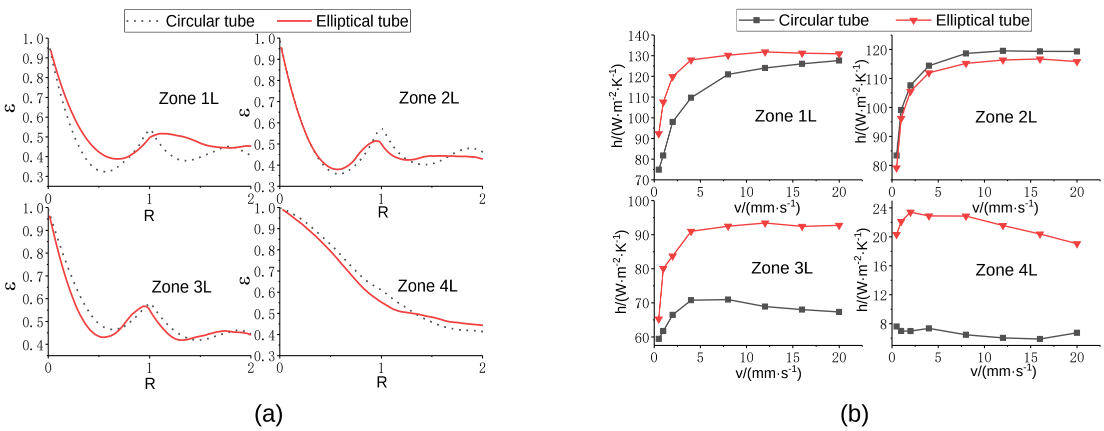

Figure 7: Comparison of porosity (a) and heat transfer coefficients (b) in different zones of two tubes

In order to carefully compare the flow and heat transfer between different zones of the two tubes, a comparison of porosity and heat transfer coefficients in different zones outside the two tubes is shown in Figure 7. Near the tube wall (R < 1 d_p) of zone 1, the porosity outside the elliptical tube is larger than that outside the circular tube. The porosity outside the elliptical tube in zone 2 is almost equal to that outside the circular tube. The porosity outside the elliptical tube in zones 3 and 4 is smaller than that outside the circular tube. The larger the porosity means that the lower filling rate of particles near the wall, which causes worse heat transfer. Compared with the flow of particles around the circular tube, the flow of particles around thee elliptical tube increases the particle velocity in zone 1, and increases the filling rate and contact number at zones 3 and 4. Therefore, the heat transfer coefficients in zones 1, 3 and 4 of the elliptical tube are higher than that of the circular tube.

4. Conclusions

In this study, the discrete element method (DEM) with heat transfer model was used to simulate the flow and heat transfer of gravity-driven particles around a circular or an elliptical tube. The main results are as follows:
1) The size of stagnation zone and cavitation zone has a significant effect on the flow and heat transfer of particle flow around the tube. The stagnation zone and cavitation zone of the elliptical tube are obviously smaller than that of the circular tube.
2) Compared with the circular tube, the filling rate in the region of $R < 2\ d_p$ outside the elliptical tube are higher. The contact number in zones 3 and 4 are 1.3 and 1.5 times of the circular tube respectively. The velocity gradient of the elliptical tube is smaller and the particle velocity in the stagnation zone is larger. Therefore, the heat transfer coefficients of the elliptical tube are higher than that of the circular tube.
3) In MBHE, elliptical tube is a better choice, but its bearing capacity need to carefully consider. As for circular tube, some optimization, such as fins at the top and bottom of the tube, is required to reduce the size of stagnation zone and cavitation zone.
In the future, convection will be added to the heat transfer model and the influence of particle size will be considered. Subsequent studies attempted to simulate multi-tube heat transfer.

Acknowledgment

The work is financially supported by National Basic Research Program of China (Grant No. 2017YFB0603500) and CSC Fellowship (No.201806285048).

References

Baumann, T., Zunft, S., 2015, Development and Performance Assessment of a Moving Bed Heat Exchanger for Solar Central Receiver Power Plants, Energy Procedia, 69, 748-757.
Duan, W., Yu, Q., Wang, Z., Liu, J., Qin, Q., 2018, Life cycle and economic assessment of multi-stage blast furnace slag waste heat recovery system, Energy, 142, 486-495.
Gen Li, T.M., 2018, Assessing China's Waste Management Activities Using a Computable General Equilibrium Model, Chemical Engineering Transactions, 63, 67-72.
Guo Z.G., Tian X, Hu Y.X., Yang J, Wang Q.W., 2018, Numerical study of heat transfer in gravity-driven particle flow nearby tube out-wall surface, Proceedings of the 16th International Heat Transfer Conference, Beijing, China, 6313-6320.
Hou, Q.F., Zhou, Z.Y., Yu, A.B., 2016, Gas–solid flow and heat transfer in fluidized beds with tubes: Effects of material properties and tube array settings, Powder Technology, 296, 59-71.
Liu, J., Yu, Q., Peng, J., Hu, X., Duan, W., 2015, Thermal energy recovery from high-temperature blast furnace slag particles, International Communications in Heat and Mass Transfer, 69, 23-28.
Subash Dhar, M.P., P R Shukla, 2018, Role of Energy Efficiency for Low Carbon Transformation of India, Chemical Engineering Transactions, 63, 307-312.
Srivastava, A., Sundaresan, S., 2003, Analysis of a frictional–kinetic model for gas–particle flow, Powder Technology, 129, 72-85.
Zhao, Z., Wang, T., Liu, P., Li, Z., 2016, A Sankey Diagram Approach to Quantifying Industrial Residual Energy in China, Chemical Engineering Transactions, 52, 37-42.
Zhang, H., Wang, H., Zhu, X., Qiu, Y.-J., Li, K., Chen, R., Liao, Q., 2013, A review of waste heat recovery technologies towards molten slag in steel industry, Applied Energy, 112, 956-966.
Zheng, B., Sun, P., Liu, Y., Zhao, Q., 2018, Heat transfer of calcined petroleum coke and heat exchange tube for calcined petroleum coke waste heat recovery, Energy, 155, 56-65.
Zhang, H., Zhou, Z., Yu, A.B., Kim, S.-Y., Jung, S.-K., 2017, Discrete particle simulation of solid flow in a melter-gasifier in smelting reduction process, Powder Technology, 314, 641-648.